REVISTA INTERDISCIPLINAR DE PESQUISA EM ENGENHARIA

CILAMCE 2016
XXXVII IBERIAN LATIN AMERICAN CONGRESS ON COMPUTATIONAL METHODS IN ENGINEERING
BRASÍLIA - DF - BRAZIL

EXPERIMENTAL EVALUATION OF SYNTHETIC INDUCTORS APPLIED IN PASSIVE SHUNT CIRCUITS TO VIBRATION MITIGATION

Bruno Gabriel Gustavo Leonardo Zambolini-Vicente

bruno.vicente@ifg.edu.br

Federal Institute of Goiás, Campus Itumbiara,

Av. Furnas, 55, CEP 75524-010, Itumbiara, Goiás, Brazil.

Antônio Marcos Gonçalves de Lima

Roberto Mendes Finzi Neto

amglima@ufu.br

finzi@ufu.br

Federal University of Uberlândia, Campus Santa Mônica,

Av. João Naves de Ávila, 2121, CEP 38400-902, Uberlândia, Minas Gerais, Brazil..

Abstract. *In the passive vibration attenuation, the electronic circuits containing synthetic impedances to resonate with a typical mechanical vibration problem is the simplest way to avoid the large volume and weight of traditional inductors, which need to be large due to low-frequency scenario of mechanics dynamics. In order to construct those simulated inductors to provide energy transfer from mechanical vibration to electrical circuit, schemes with operational amplifiers are used, that deliver high values of henrys with formation law depending of resistors and capacitors connected to these amplifiers. In this study it was held the experimental evaluation of circuits employing three kinds of synthetics inductors, configurable between serial and parallel arrangements, applying three types of shunts circuits described in the literature, tuned to mitigate three modes of a structure. The results were organized to provide an overview of the attenuation capability, showing the impact of circuit tunings for each vibrate mode. Thus, the experiments indicate, for example, that for the rated circuits, the tuning with the greatest attenuation is Wu Parallel when setup to the first mode. Overall, the results point to a potential attenuation capability, that can be further enhanced from the use of other circuits more adapted in the literature.*

Keywords: *Passive Vibration Control, Experimental Evaluation, Passive Shunt Circuit, Synthetic Inductor.*

1 INTRODUCTION

In literature of passive vibration control of smart structures, papers such as Moheimani (2003) and Soltani *et al.* (2014) describes from the fundamentals to recent advances in theory related to the use of electrical circuits coupled to piezoelectric vibration mitigation. With regard to passive circuits in which there is no directly power insert to control vibration, one possibility is the use of tuned electrical impedance to resonate with the electrical impedance generated by a piezoelectric coupled to the structure, in order to maximize the effect energy transfer via electromechanical coupling. To this end, the papers of Hagood & von Flotow (1991), Wu (1996) and Wu & Bicos (1997) presented the first development of theories for passive circuits and demonstrated the need for large inductance values (values above mH) to balance the capacitive nature of the piezoelectric wafer at low frequency, which in practice is only feasible through the use of synthetic inductors, since the traditional methods of construction inductors require large volumes and prohibitive addition of mass (Sedra, 2009). More recently, the work of Yamada *et al.* (2010) showed significant differences in the calculation of tunings of resistors and inductors for shunts circuits, with distinction of values when using compliance, mobilitance or accelerance. From the experimental point of view, works like developed by Behrens et al. (2003) and Thomas et al. (2012) reported the use of synthetic inductors vibration control schemes, but little or no discussion about the different possibilities for such circuit inductors, as well as the performance mode or attenuation level are exposed. Thus, this work presents the experimental evaluation of the performance of a monomodal shunt circuit for attenuating vibrations, which were combined three types of topologies with three types of synthetic inductors, evaluated in three different modes of vibration. For this task, a clamped-free aluminum beam was used as a host structure for a piezoelectric coupled to the shunt circuit, illustrated in Fig. 1.

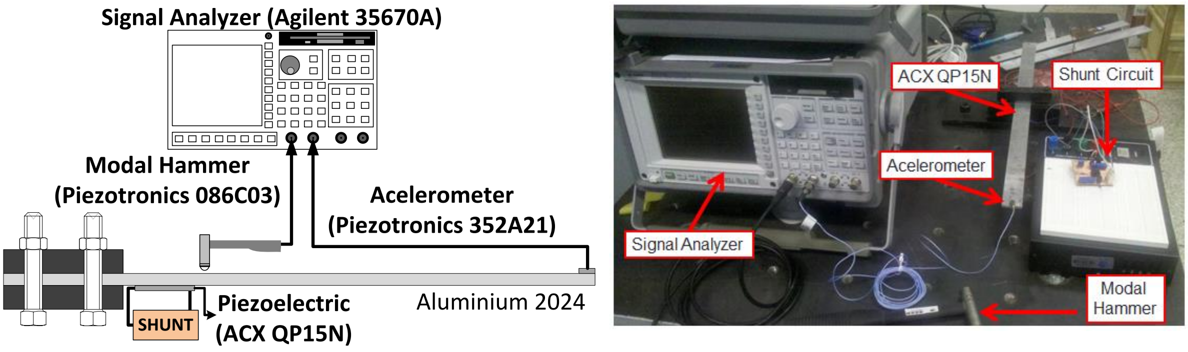

a) b)

Figure 1: a) Schematic of test b) Experimental assembly.

2 ELETROMECHANICAL DYNAMICS

In their pioneering paper, Hagood and von Flotow (1991) have demonstrated that through the elementary mass and stiffnesses matrices for both mechanical, electrical and electromechanical coupling effects it is possible to construct the following equation of motion of a structure incorporating piezoelectrical elements by using standard procedure:

$$\begin{bmatrix} \boldsymbol{M}_{uu} & 0 \\ 0 & 0 \end{bmatrix} \begin{Bmatrix} \ddot{\boldsymbol{u}}_g \\ \ddot{\boldsymbol{\phi}}_g \end{Bmatrix} + \begin{bmatrix} \boldsymbol{K}_{uu} & \boldsymbol{K}_{u\varphi} \\ \boldsymbol{K}_{\varphi u} & \boldsymbol{K}_{\varphi\varphi} \end{bmatrix} \begin{Bmatrix} \boldsymbol{u}_g \\ \boldsymbol{\phi}_g \end{Bmatrix} = \begin{Bmatrix} \boldsymbol{F}_g \\ \boldsymbol{Q}_g \end{Bmatrix} \tag{1}$$

where u_g and Φ_g are the vectors of displacements and electrical potential respectively; F_g and Q_g are the vectors of imposed forces and electrical charges; K_{uu} is the purely mechanical stiffness matrix, $K_{u\varphi} = K_{\varphi u}^T$ are the eletromechanical stiffness matrices and $K_{\varphi\varphi}$ is the purely electrical stiffness matrix. Moreover, considering the analysis in the frequency domain (neglecting the initial conditions), Eq. (1) assumes the form:

$$\left(\boldsymbol{K}_{uu} - \omega^2 \boldsymbol{M}_{uu}\right)\boldsymbol{U}(\omega) + \boldsymbol{K}_{u\varphi}\boldsymbol{\Phi}(\omega) = \boldsymbol{F}(\omega) \tag{2a}$$

$$\boldsymbol{K}_{\varphi u}\boldsymbol{U}(\omega) + \boldsymbol{K}_{\varphi\varphi}\boldsymbol{\Phi}(\omega) = \boldsymbol{Q}(\omega) \tag{2b}$$

Thus, the equations of motion must be modified in order to consider the shunt circuit. According to Ohm's law, the relationship between flow of charges and electric potential, which depends on the electrical impedance Z(ω), can be written in the frequency domain as:

$$\boldsymbol{Q}(\omega) = \frac{1}{j\omega} Z^{-1}(\omega)\boldsymbol{\Phi}(\omega) \tag{3}$$

Proceeding the elimination of Q(ω) by combining Eqs. (2b) and (3) and replacing Φ(ω) resultant in Eq. (2a), it is possible to obtain the frequency response function (FRF) of Eq. (4):

$$\boldsymbol{H}(\omega) = \left[\boldsymbol{K}_{uu} - \boldsymbol{K}_{u\varphi}\left(\boldsymbol{K}_{\varphi\varphi} - \frac{1}{j\omega}Z^{-1}(\omega)\right)^{-1}\boldsymbol{K}_{\varphi u} - \omega^2\boldsymbol{M}_{uu}\right]^{-1} \tag{4}$$

Apart from mechanical, electrical and electromechanical terms, the Eq. (4) show the influence of electrical shunt circuit in the system's FRF, introduced by its impedance Z(ω).

3 SHUNTS CIRCUITS TOPOLOGIES

For the shunt circuit lodged at the Fig.1 and in which its effect is pointed in the FRF electromechanical system, Eq. (4), three of the widely held topologies circuits and their tunings were tested: a series, in which the shunt impedance circuit assumes $Z(\omega) = R + \omega L$, and two parallel, with impedance equal to $Z(\omega) = \omega RL/(R + \omega L)$, showed in Table 1:

Table 1 - Topologies and their equations to tune the parameters of the shunt circuits evaluated..

Topology	Tuning equations for R and L		
	$R = \frac{\sqrt{2}K_{ij}}{C_{PZT}\omega_n\left(1 + K_{ij}^2\right)}$	$L = \frac{1}{C_{PZT}\left(1 + K_{ij}^2\right)\omega_n^2}$	Hagood e von Flotow Serie (Hagood & von Flotow, 1991)
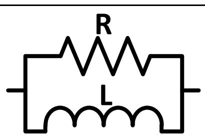	$R = \frac{1}{\sqrt{2}K_{ij}C_{PZT}\omega_n}$	$L = \frac{1}{C_{PZT}\left(1 - \frac{K_{ij}^2}{2}\right)\omega_n^2}$	Hagood e von Flotow Parallel (Hagood & von Flotow, 1991)
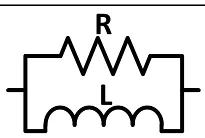	$R = \frac{1}{2.828\pi f_s C_{PZT}^C\, K_{ij}}$	$L = \frac{1}{C_{PZT}^C(2\pi f_s \alpha)^2}$	Wu e Bicos Parallel (Wu & Bicos, 1997)

Where $K_{ij} = \sqrt{f_n^2 - f_s^2}/f_s$ is the generalized electromechanical coupling factor, $\alpha = (1 - K_{ij}^2/2)^{1/2}$ is the optimum normalized tuning frequency, C_{PZT}^C is the capacitance value after adhered to structure (Wu & Bicos, 1996), C_{PZT} It is the capacitance of the piezoelectric measured outside the structure, in the case of ACX QP15N, the value measured was C_{PZT}=75,3nF, ω_n is the natural frequency in rad/s (and f_n em hertz) for piezo in open circuit state and f_s is the natural frequency (in hertz) to piezoelectri short-circuit condition.

4 SYNTHETIC INDUCTORS

The topologies to be implemented as a shunt circuit described in Table 1 were constructed using as synthetic inductors schemes described by Tellegen (1948), termed as gyrator and Riordan circuit (1967) and Antoniou (1969) depicted in Fig. 2. In these circuits, the operational amplifier, the capacitor and associated resistor causing, in schematic terminals, the shift of almost 90 ° of phase voltage, resulting in the required function of an inductor. According to literature, the value of the simulated inductance in *gyrator* scheme takes $L=R_1R_2C_3$, with R_1 adjustable, while in Riordan and Antoniou's circuits assumes $L=(R_1R_3C_3R_5)/R_2$ in both configurations, in which case being R_3 the adjustable resistor.

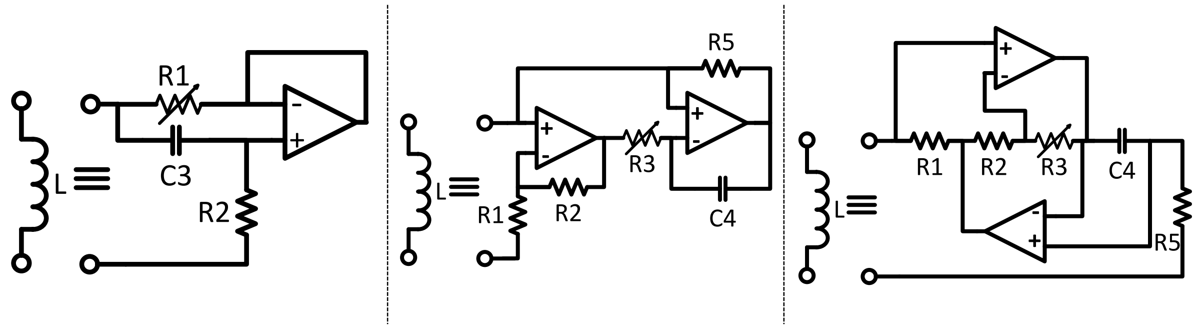

a) b) c)

Figure 2 – Synthetic inductors circuits: a) *gyrator*, b) Riordan, c) Antoniou.

Below, Fig. 3 exhibits the PCB Design - Printed Circuit Board, its 3D design and the finished PCB, for the investigated mono-modal shunts. It is emphasized that the PCBs allow independent adjustment of both the inductance value via adjustable resistors R_1 (gyrator) or R_3 (Riordan and Antoniou), and adjusting the shunt tune resistor *R* (Table 1), besides allowing the reconfiguration of the topology series and parallel listed in Table 1.

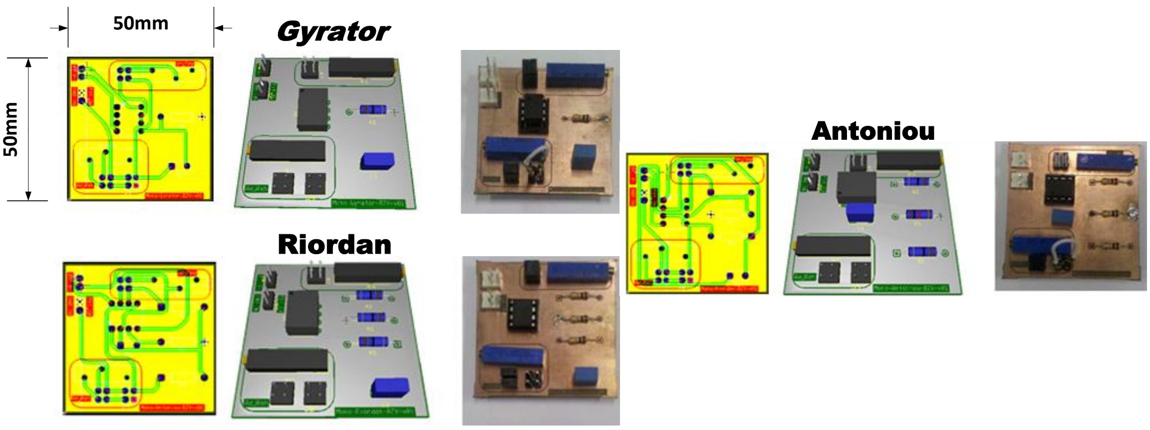

Figure 3 –Mono-modal shunt circuits *gyrator*, Riordan and Antoniou: from PCB design to PCB finished.

5 EXPERIMENTAL EVALUATION

Based on the presented experimental setup in Fig. 1, the procedures were carried out described in Hagood & von Flotow (1991) and Wu & Bicos (1997) for *R* and *L* of tune, applying to the Table 1 equations, obtaining thus Table 2. It should be noted that f_n e f_s, open circuit and short-circuit frequencies, must be obtained leaving the piezoelectric structure set in open circuit and with their short-circuit terminals, respectively. The frequencies ω_n e ω_{sc} are the frequencies f_n e f_s in rad/s and the capacitance $\boldsymbol{C_{PZT}^C}$ must be measured with the piezoelectric already glued to the structure.

Table 2 - Topologies and their tunings of shunts circuits evaluated.

	Hagood & von Flotow Series Tuning						
	Unshunted Frequencies		Natural/Short Cicuit Freqs		Coupling Factor	Resonant Circuit Parameters	
	f_n [Hz]	f_{sc} [Hz]	ω_n [rad]	ω_{sc} [rad]	K_{31} [ad]	R [Ω]	L [H]
Mode #1	31.690	31.940	199.114	200.685	0.125	11600	329.82
Mode #2	194.80	194.90	1223.96	1224.59	0.032	491.00	8.856
Mode #3	530.50	531.10	3333.23	3337.00	0.048	267.10	1.193

	Hagood & von Flotow Parallel Tuning						
	Unshunted Frequencies		Natural/Short Cicuit Freqs		Coupling Factor	Resonant Circuit Parameters	
	f_n [Hz]	f_{sc} [Hz]	ω_n [rad]	ω_{sc} [rad]	K_{31} [ad]	R [kΩ]	L [H]
Mode #1	31.690	31.940	199.114	200.685	0.125	377.7	337.59
Mode #2	194.80	194.90	1223.96	1224.59	0.032	239.5	8.869
Mode #3	530.50	531.10	3333.23	3337.00	0.048	59.29	1.197

	Wu & Bicos Parallel Tuning						
	Unshunted Frequencies		Capacitance after glued	Normalized Opt. Freq.	Coupling Factor	Resonant Circuit Parameters	
	f_n [Hz]	f_{sc} [Hz]	C_{PZT}^C [nF]	α [ad]	K_{31} [ad]	R [kΩ]	L [H]
Mode #1	31.690	31.940	65.54	0.996	0.125	430.6	381.82
Mode #2	194.80	194.90	65.54	1.000	0.032	275.1	10.179
Mode #3	530.50	531.10	65.54	0.999	0.048	68.05	1.372

Beginning in the *R* and *L* tuning values listed in Table 2, took place for all three modes in each of the three tunings, for each of the three circuits, in the three piezoelectric connection conditions (open circuit short circuit and connected shunt circuit), the experimental evaluation of 81 FRFs, resulting from all possible combinations in impact test of 30 averages, with 1600 acquisition points in FRFs, with frequency band from 0 to 800Hz, always with controlled temperature 24°C. Thus, Fig. 4 illustrates two such FRFs as an example of the results obtained:

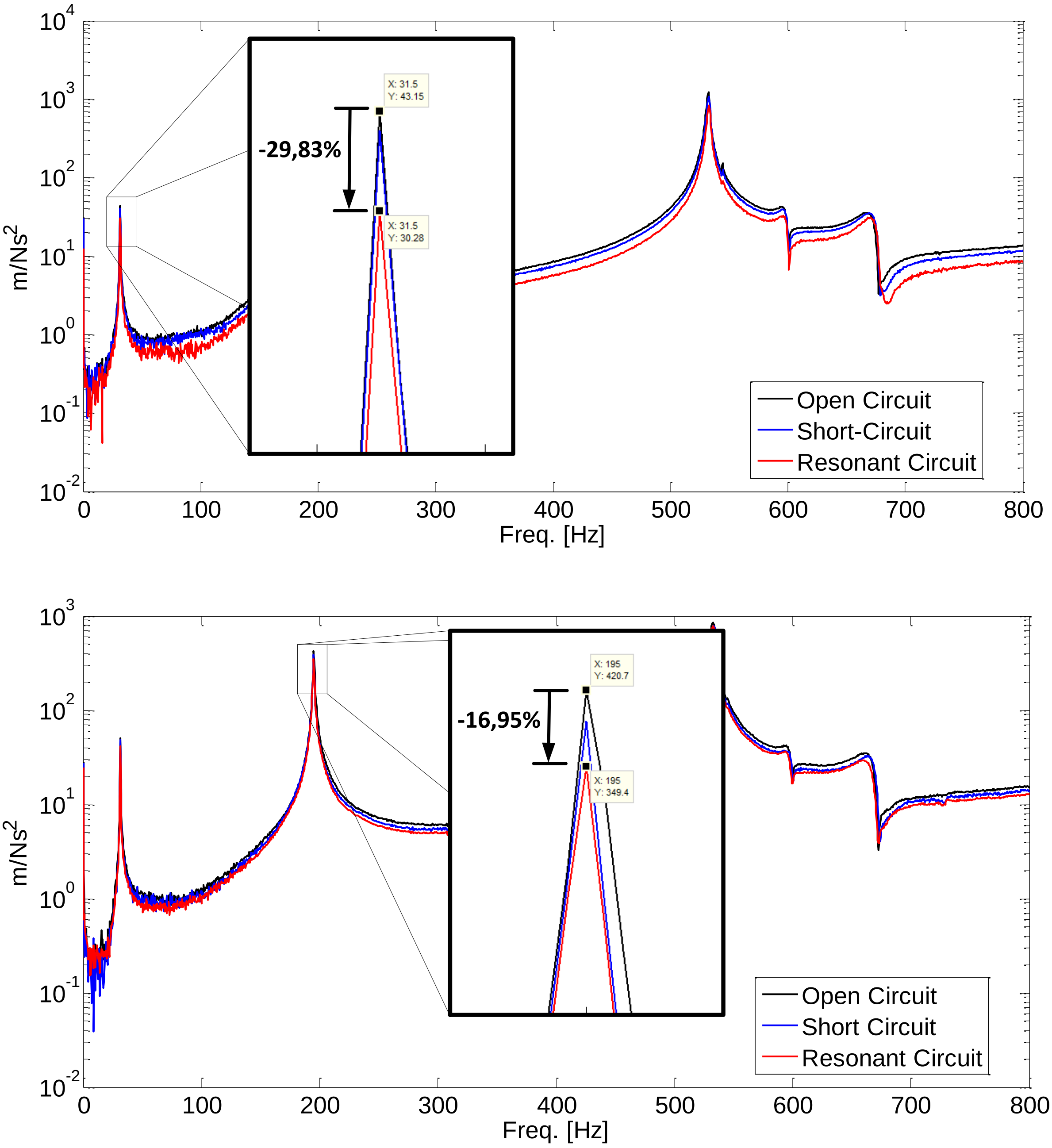

Figure 4 – Examples of FRFs obtained: above topology Wu & Bicos parallel with inductor Antoniou, tuned in Mode #1; below topology Hagood & von Flotow parallel with gyrator inductor tuned in Mode #2.

Following, Table 3 shows the summary table of all the reduction levels achieved for all arrangements topologies/inductors/modes. The comparative FRF amplitudes were established for the open piezoelectric and amplitude values are in m/Ns^2.

Table 3 – Decreasing amplitudes for all combinations of topologies, inductors and evaluated modes.

		Gyrator			Riordan			Antoniou		
Hagood & von Flotow Serie		Open Circuit	Reson. Circuit	% ↓	Open Circuit	Reson. Circuit	% ↓	Open Circuit	Reson. Circuit	% ↓
	#1	48,68	42,50	12,70	45,12	35,22	21,94	41,89	34,81	16,90
	#2	448,4	406,3	9,39	402	350,1	12,91	413,8	342,6	17,21
	#3	965,2	916,9	5,00	983,2	886,5	9,84	1002	906,5	9,53
Hagood & von Flotow Parallel		Open Circuit	Reson. Circuit	% ↓	Open Circuit	Reson. Circuit	% ↓	Open Circuit	Reson. Circuit	% ↓
	#1	48,68	43,42	10,81	46,03	34,87	24,25	43,57	35,15	19,33
	#2	420,7	349,4	16,95	404,9	352,8	12,87	419,8	340,9	18,79
	#3	967,2	897,9	7,17	980,2	882,6	9,96	999,8	905,6	9,42
Wu & Bicos Parallel		Open Circuit	Reson. Circuit	% ↓	Open Circuit	Reson. Circuit	% ↓	Open Circuit	Reson. Circuit	% ↓
	#1	48,68	45,59	6,35	46,48	34,16	26,51	43,15	30,28	29,83
	#2	422,7	357,4	15,45	422,8	360,9	14,64	420,2	339,2	19,28
	#3	957,2	875,1	8,58	998,7	913,1	8,57	994,8	907,9	8,74

6 RESULTS AND DISCUSSION

Through the consolidated data in Table 3, the results were organized in *Average Decrease Amplitude per Synthetic Inductor*, *Average Decrease Amplitude per Topology* and *Average Decrease Amplitude per Vibrate Mode*, as can be seen in Fig. 5-7.

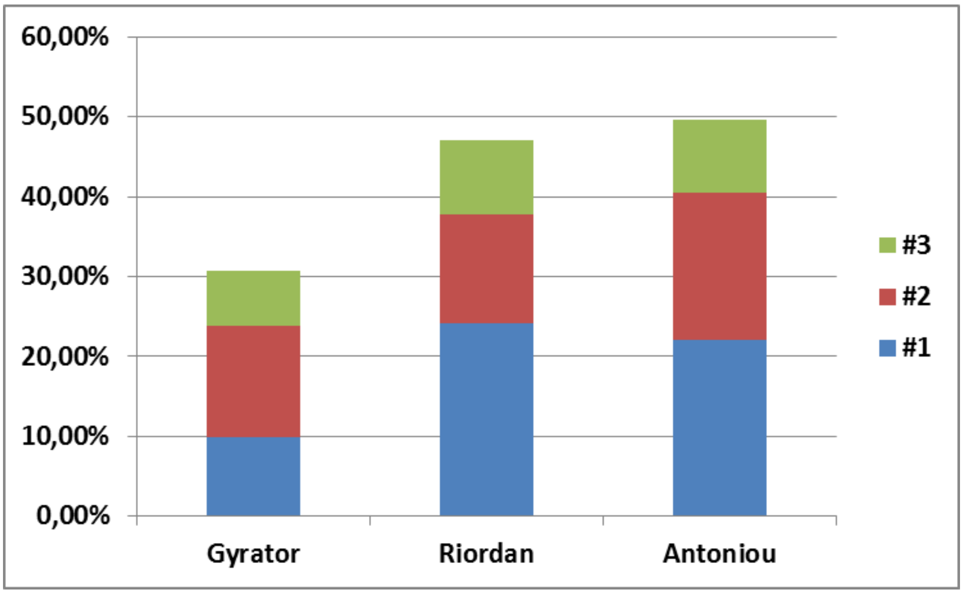

Figure 5 – Average decrease of amplitude per type of synthetic inductor *versus* vibration modes.

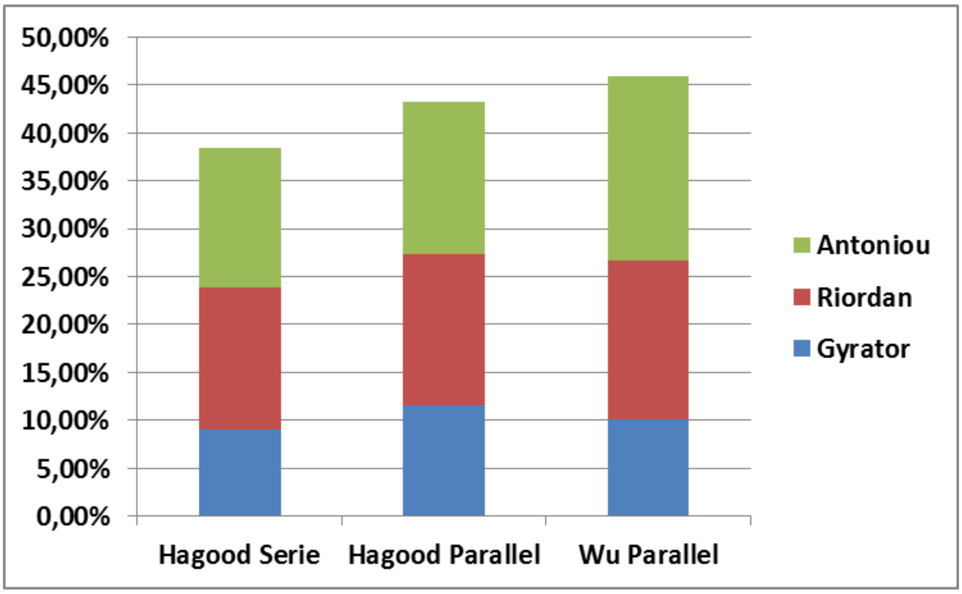

Figure 6 – Average decrease of amplitude per topology *versus* type of synthetic inductor.

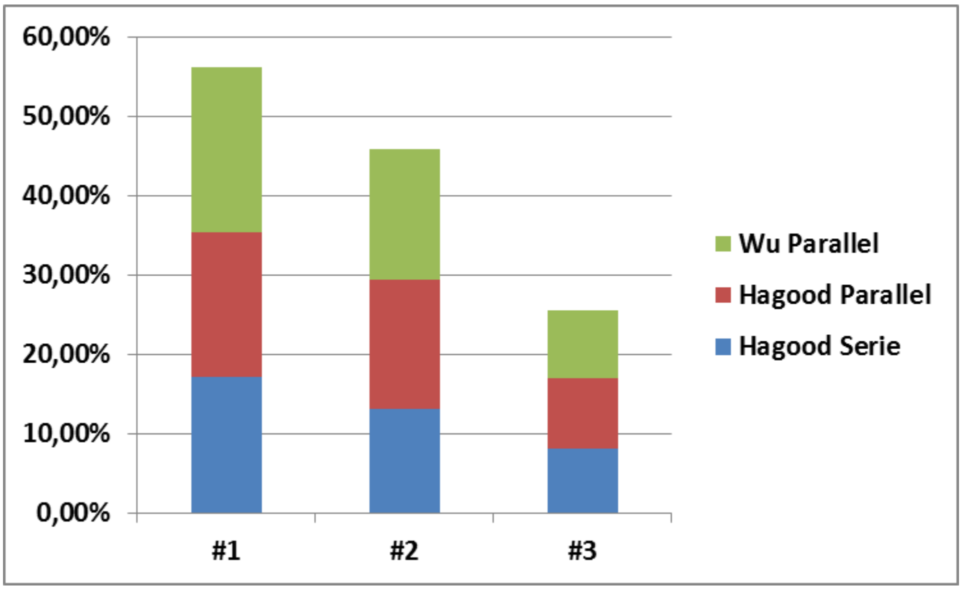

Figure 7 – Average decrease of amplitude per vibration mode *versus* topologies.

The analysis of results provides the following conclusions:

- Observing the Fig. 5, the Antoniou and Riordan circuits have similar performance to the 3rd mode, being based Antoniou best inductor for 2nd mode and Riordan better for the 1st vibrate mode. If the interest is to attenuate more, regardless of the mode, then the solution is given using Antoniou. Furthermore, it should be noted good performance scheme gyrator inductor for 2nd mode higher than the obtained with inductor Riordan.
- Focusing on topology (Fig. 6), it can be said that Wu Parallel is the compromise solution, delivering maximum reduction for the 2nd mode and 3rd mode, slightly lower than the Hagood Parallel on 1st mode.

- About the attenuation point of view modes (Fig. 7), it is evident that the largest reduction achieved appears to 1st mode in all topologies. Observing the 2nd mode, it can be affirmed, however, that Hagood parallel configuration has a lower reduction performance than the others. In addition to the 3rd mode, all topologies have practically the same level of reduction. Generally all modes, again note that the performance tuning Parallel Wu shows slight superiority.

7 CONCLUSIONS

In summary, the experimental investigation of mono-modal circuit indicates that the tuning Wu Parallel provides better reduction than the others, this results in a way discussed in own Wu & Bicos work (1997). As for the best circuit for synthetic inductor, at first Riordan inductor figure how best candidate, followed closely by Antoniou inducer. Moreover, on the underperformance of topology Hagood Series, it can be affirmed that parasite resistance problems may be present in the circuit, which has been reported and investigated in the work Viana & Steffen Jr. (2006), as well as solutions involve adding more operational amplifiers to limit the effect was proposed by Yuce & Minaei (2009).

ACKNOWLEDGEMENTS

The first author (B.G.G.L. Zambolini-Vicente) devotes a special thanks to the Federal Institute of Goiás for the financial support. The authors are grateful to the Brazilian Research Council – CNPq for the continued support to their research works, especially through research projects 308310/2010-1 (A.M.G. de Lima). The authors express their acknowledgements to the Minas Gerais State Agency FAPEMIG for the financial support to their research activities and the National Institute of Science and Technology of Smart Structures in Engineering – INCT–EIE , jointly funded by CNPq, CAPES, FAPEMIG and PETROBRAS.

REFERENCES

Antoniou, A., 1969, Realization of Gyrators using Operational Amplifiers, and their use in RC-Active-Network Synthesis, *IEEE Proc., Vol. 116, Nº11, pp. 1838-1850.*

Behrens, S. Moheimani, S. O. R., Fleming, A. J., 2003, Multiple mode current flowing passive piezoelectric shunt controller, *Journal of Sound and Vibration 266 (2003) 929–942.*

Hagood, N. W. and Flotow, A. H. V., 1991. Damping of structural vibrations with piezoelectric materials and passive electrical networks. *Journal of Sound and Vibration, Vol. 146, pp. 243-268*.

Moheimani, S. O. R., 2003. A Survey of Recent Innovations in Vibration Damping and Control Using Shunted Piezoelectric Transducers. *Transactions On Control Systems Technology, Vol. 11, No. 4, July 2003, IEEE*.

Riodan, R. H. S., 1967. Simulated inductors using differential amplifiers. *Electron. Lett., vol. 3, no. 2, pp. 50–51.*

Sedra, A. S.; Smith, K. C. *Microeletrônica*. 6ª Edição / Editora: Oxford.

Soltani, P., Kerchen, G., Tondreau, G., Deraemaeker, A., 2014. Piezoelectric vibraion damping using resonant shunt circuits: an exact solution. *Smart Materials and Structure 23, 125014 (11pp)*.

Tellegen, B. D. H., April 1948. The gyrator, a new electric network element. *Philips Res. Rep. 3: 81–101*.

Thomas, O., Ducarne, J., Deü, J-F., 2012. Performance of piezoelectric shunts for vibration reduction. *Smart Materials and Structures, 21,015008 (16pp).*

Viana, F.A.C., Steffen JR., V., 2006. Multimodal vibration damping through piezoelectric patches and optimal resonant shunt circuits. *Journal of the Brazilian Society of Mech. Sciences and Engi., Vol.28, No.3,pp.293–310*.

Wu, S. Y., 1996. Piezoelectric shunts with parallel R-L circuit for structural damping and vibration control. *inProc. SPIE Smart Structures and Materials, Passive Damping and Isolation, vol. 2720, SPIE, Mar. 1996, pp. 259–269.*

Wu, S., Bicos, A. S., 1997. Structural vibration damping experiments using improved piezoelectric shunts. *SPIE Smart Structures and Materials, Passive Damping and Isolation Vol. 3045.*

Yamada, K., Matsuhisa, H., Utsuno, H., 2010. Optimum tuning of series and parallel LR circuits for passive vibration suppression using piezoelectric elements. *Journal of Sound and Vibration, Vol. 329, (24) (2010) 5036–5057*.

Yamada, K., Matsuhisa, H., Utsuno, H., 2013. Enhancement of efficient of vibration suppression using piezoelectric elements and LR circuit by amplification electrical resonance. *Journal of Sound and Vibration, Vol. 333, Nov. 2013, pp 1281-1301*.

Yuce, E., Minaei, S., 2009. On the Realization of Simulated Inductors with Reduced Parasitic Impedance Effects. *Circuits Syst Signal Process 28: 451–465.*